Watershed Ecology and the Environment 5 (2023) 46–55

Contents lists available at ScienceDirect

Watershed Ecology and the Environment

journal homepage: www.keaipublishing.com/wsee

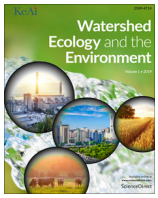

Detection of land use/land cover changes in a watershed: A case study of the Murredu watershed in Telangana state, India

Padala Raja Shekar *, Aneesh Mathew

Department of Civil Engineering, National Institute of Technology, Tiruchirappalli 620015, Tamil Nadu, India

ARTICLE INFO

Article history:
Received 20 November 2022
Revised 14 December 2022
Accepted 14 December 2022
Available online 20 December 2022

Keywords:
Land use land cover
Remote sensing
Geographic information system
Murredu watershed

ABSTRACT

Land-use change refers to a change in how a particular area of land is utilised or managed by humans. Land-cover change refers to a change in some continuous features of the land, such as vegetation type, soil conditions, and so on. For the purpose of identifying change-vulnerable areas and creating sustainable ecosystem services, mapping and quantifying the state of land use/land cover (LULC) changes and change-causing factors are crucial. The present research utilizes a geographic information system (GIS) and remote sensing (RS) techniques to categorise and identify changes in a Murredu watershed in Telangana state, India, between 1996 and 2019. Five major LULC categories (agricultural land, forest, barren land, built-up area, and waterbodies) from satellite images of 1996 to 2019 were mapped. The maximum likelihood approach was used to supervise the classification process, and high-resolution Google Earth Pro was used to evaluate the accuracy of the classified map. The accuracy of the mapping was evaluated using the error matrix and Kappa statistics. Overall classification accuracy for the classified image of 2019 was found to be 90 % with overall kappa statistics of 85.98%. From these findings, change detection analysis shows that the area used for agricultural land, barren land, forest, built-up areas, and waterbodies has increased by 5.17%, 3.39%, 0.84%, and 0.26%, respectively, between 1996 and 2019. The forest area has decreased by 9.67% at the same time. Therefore, this research anticipates that the findings might provide information to planners, land managers, and decision-makers for the sustainable management and development of the natural resource.

1. Introduction

The term "land-use" describes how humans use the land cover to support themselves. It covered both the methods and motivations used to change the biophysical characteristics of the land. Crop cultivation, mining, housing, and infrastructure development are a few examples of land use (Lambin and Geist, 2006). Contrarily, the term "land-cover" refers to the biophysical state of the earth's surface and the immediate subsurface, which includes human alterations, topography, and soil like infrastructures (Lambin et al., 2006). Changes in a specific type of land use or land cover's areal extent (increases or decreases) are referred to as LULC changes. Ecosystem, hydrological, and climate modelling as well as decision-makers might use the spatial and temporal data on LULC to analyse the effects of LULC on local climate, water supplies, and biogeochemical cycles in terrestrial ecosystems (Tian et al., 2014; Chen et al., 2021; Meer and Mishra, 2020).

The hydrological and geomorphological processes and features of a river system, as well as their interactions, variability, and spatial distribution, are described by river hydro-morphology (Akpoti et al., 2016; Javed et al., 2011; Shekar and Mathew, 2022c; Redvan and Mustafa, 2021; Mathew and Shekar, 2023; Subba Rao et al., 2016). It deals with the physical mechanisms that control river behaviour and the morphology that results from those mechanisms (Hajdukiewicz et al., 2017; Subba Rao, 2016). Through flooding, peak flow, and evaporation that are either increased or decreased as a result of LULC change, the components of the water balance are altered (Teklay et al., 2021; Santillan et al., 2019). In addition to LULC modification, morphological features are impacted by adjustments to water balance factors such peak flows (Javed et al., 2009; Langat et al., 2020; Hassaballah et al., 2017; Serra et al., 2008). Given that it determines the status of the soil, land cover is significant in these processes (Chakilu and Moges,

Abbreviations: LULC, Land use/land cover; GIS, Geographical information system; RS, Remote sensing; SRTM, Shuttle radar topography mission; DEM, Digital elevation model; USGS, United States Geological Survey; Km, Kilometre; %, Percentage.

* Corresponding author.
E-mail address: rajashekar.padala873@gmail.com (P. Raja Shekar).

https://doi.org/10.1016/j.wsee.2022.12.003
2589-4714/

2017; Abebe et al., 2022). The scale of these effects varies according to the features of the watershed, such as its weather, soil properties, degree of change, and size (Allan et al., 1997; Kayitesi et al., 2022).

Finding differences in a phenomenon's status by watching it at various periods is the method of "change detection" (Singh, 1989). Land degradation and desertification (Gao and Liu, 2010; Shekar and Mathew, 2023), deforestation (Wyman and Stein, 2010; Schulz et al., 2010), and other cumulative changes are only a few examples of how change detection is helpful in applications connected to LULC changes (Nagendra et al., 2006; Belay and Mengistu, 2019; Mathew et al., 2022).

Assessment of LULC change aids in determining the degree of human impact over the environment. Numerous academics believed it to be a significant process that has local, regional, and worldwide effects on both natural environments and socioeconomic conditions (Wubie et al., 2016). The majority of the time, LULC changes are caused by anthropogenic activities such as tree cutting, land conversion to agriculture, and human settlement, all of which disrupt biodiversity, water and radiation budgets, have an impact on trace gas emissions, and other processes that have an impact on the biosphere and climate (Rawat and Kumar, 2015; Subba Rao, 2012). As a result, knowledge of LULC is becoming more and more important for managing both the environment and living situations (Subba Rao and Prathap Reddy, 2004).

Due to its recurring data collecting, precise georeferencing processes, and digital format suited for computer processing, satellite remote sensing is the most popular data source for the quantification, identification, and mapping of LULC forms and variations (Chen et al., 2005; Subba Rao, 2006). Several multi-date images are used in remote sensing change detection and monitoring to assess LULC variations between image acquisition dates caused by diverse environmental conditions and human activity (Singh, 1989; Subba Rao et al., 2022). Application of satellite remote sensing for LULC change detection requires a thorough understanding of landscape features, imaging technology, and methodology used in relation to the purpose of the study (Yang and Lo, 2002).

There are several satellite programmes running right now. The Landsat programme is exceptional for change detection research because it offers a historical and ongoing archive of imagery (Mohamed et al., 2020; Nageswara Rao et al., 2018; Subba Rao, 2003). For the mapping, monitoring, and management of LULC, Landsat images may be processed to reflect land cover over enormous regions and over extended periods, which is new and critically essential (Wulder et al., 2008; Kogo et al., 2019). Landsat data have been used in a number of studies to address LULC variations, some of which focused on semi-arid and arid regions.

In the watershed, biological circumstances, gradients, and elevations play a significant role in determining land use/land cover. In addition to the aforementioned variables, technological, socioeconomic, and institutional setup are also anticipated to have an impact on the LULC change (Rai et al., 1994). It has become vital to have an inventory of the land resources in a watershed due to the growing possibility of anthropogenic change and its effects on the environment (Javed et al., 2009; Shekar and Mathew, 2022b; Subba Rao, 2009; Subba Rao, 2011).

In the present work, the changing pattern of LULC in the Murredu watershed from 1996 to 2019 has been mapped using multitemporal satellite images from Landsat-5 TM and Landsat 8 OLI/TIRS imagery. The main objective of the current study was to utilise GIS and RS applications to find out the extent of changes occurring in the Murredu Watershed. However, the specific objectives were to: utilize SRTM-DEM to delineate the Murredu basin's watershed; and, furthermore, detect LULC changes in the Murredu watershed between 1996 and 2019.

2. Study area

The current investigation was carried out in the Telangana state of India's Murredu watershed (Fig. 1). At latitudes 17° 10′ 0″ and 17° 50′ 0″ North and longitudes 80° 20′ 0″ and 80° 50′ 0″ East, the watershed is located and covering over 1593 km^2 in area. The Shuttle radar topography mission (SRTM) Digital elevation model (DEM) determines that the Murredu River basin is situated between 57 and 784 m above sea level. The current study region has two different types of important rocks, according to the United States Geological Survey's (USGS) World Geologic Maps. The geological ages of two rocks are Lower Triassic to Upper Carboniferous and undivided Precambrian (Shekar and Mathew, 2022a). The major soil classes of the area, according to FAO soil classification (1988), are clay loam, and clay.

3. Data acquisition

The SRTM-DEM data, collected and was utilized to generate watershed boundary of the Murredu basin. For the purpose of visual image interpretation and identifying LULC change, satellite data comprised of multi-spectral data collected by the Landsat satellite and made available by the USGS Earth Explorer (https://earthexplorer.usgs.gov/) were utilised (Table 1). Land cloud cover and scene cloud cover of images should be less than ten percentage were selected as criteria during image selection because their presence could significantly lower the accuracy of the categorization task.

The Landsat-8 image acquired in 2019 is part of the utilised satellite dataset. Launched on 2013, the Landsat-8 satellite sensor has two sensors: a thermal infrared sensor (TIRS) and an operational land imager (OLI). Landsat-8 satellite information consist of eleven bands with a spatial resolution of 30 m for bands 1 through 9. For bands 10 as well as 11, the spatial resolution is 100 m. In the panchromatic band (band 8), which has a spatial resolution of 15 m. Bands 1 to 7 coastal, blue, green, red, near-infrared, shortwave infrared I, and shortwave infrared II were chosen for examination in this study since bands 8 to 11 are less frequently employed in LULC classification (https://www.usgs.gov/media/images/landsat-8-band-designations).

On the other hand, the satellite dataset used includes the 1996 Landsat-5 image. Landsat-5 Thematic Mapper (TM) level 1 records were acquired in 1996; the mission was launched on 1984. Each of the seven bands of the Landsat-5 satellite data has a spatial resolution of 30 m. Thermal band 6 has a 120 m spatial resolution. Visible (bands 1 to 3), near-infrared, and mid-infrared are included (https://www.usgs.gov/landsat-missions/landsat-5). It was difficult to choose images from the same date across the entire study period. Additionally, LULC class ground truth data were used. This information was gathered as reference data points for 2019 image analysis utilising the Google Earth Pro, and it was utilised to classify images and evaluate the classification results' overall accuracy.

4. Data preparation for watershed delineation

The highest sensitivity zones may be extrapolated using DEMs, which are based on watershed realisation utilising the computational watershed application of Spatial Analyst tools (Metz et al., 2011; Subba Rao et al., 2001). This study made use of the SRTM-DEM (SRTM 1 Arc Second) at a spatial resolution of 30 m. The first step after importing the DEM file into ArcGIS 10.7 is projecting the DEM into a co-ordinate system. Since elevation data sinks are frequently the result of data inaccuracies, it is crucial to eliminate all depressions or sinks from the DEM layer using the fill function. The DEM is used to construct the flow direction raster, which depicts

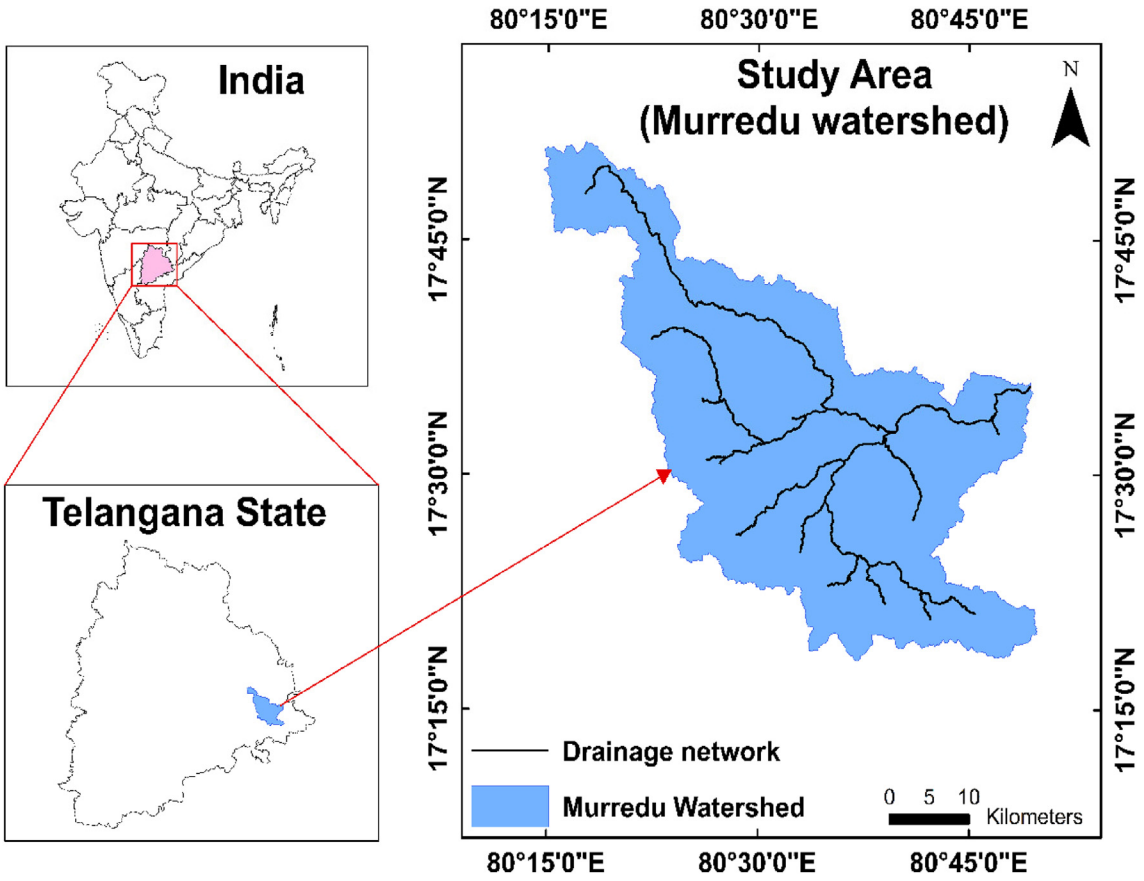

Fig. 1. Study map of the Murredu watershed.

Table 1
Information about the satellite image that was used in the investigation.

Sensor category	Scene Path/ Row	Date Acquired	Scene Path/ Row	Date acquired	Spatial resolution	Source
Landsat TM 5	143,48	Nov. 17, 1996	142,48	Nov. 10, 1996	30 m	USGS
Landsat OLI/TIRS 8	143,48	Nov. 17, 2019	142,48	Nov. 10, 2019	30 m	USGS

the real direction of water flow. A Stream Network, which is defined by Flow Accumulation, is produced when the grid is converted into a linear vector file (shapefile) using ArcGIS' Stream to Feature tool. Run "Snap Pour Point" to snap the pour points to the closest point of maximal flow accumulation after extracting stream instructions (outlet). Use the hydrology toolbox's Watershed function to delineate watershed. Convert the Watershed layer's format from raster to polygon (vector). Fig. 2 depicts the flow chart used for watershed delineation.

5. Methodology

Fig. 3 displays the whole methodology framework and data analysis. The study's full methodology is listed below.

5.1. Pre-processing

Prior to change detection, pre-processing of satellite images is crucial and has the specific objective of creating a more direct connection between biophysical processes and information (Coppin et al., 2004; Kayitesi et al., 2022). The bands were combined into a single layer using layer stacking of the ERDAS IMAGINE 2015 software for image processing and execution supervised classification of the satellite images. Then, using ArcGIS 10.7, the shapefile of the Murredu watershed area that was generated as a result of the watershed delineation procedure was used to extract these images. For mapping, a uniform false colour composite was made for each image.

5.2. Land-cover classification scheme

A classification scheme that specifies the LULC classes was taken into consideration when creating the LULC map from satellite imagery. The ideal number of LULC classes depends on the specifications of a particular project for a particular application. For mapping the entire watershed region, the five key LULC classifications of built-up area, agricultural land, forest, barren land, and waterbodies were selected (Table 2).

5.3. Post-processing

Delimiting polygons around typical sites allowed training samples to be chosen for each of the specified LULC types. The spectral signatures for the various land cover categories seen in the satellite images were determined using the pixels contained in these polygons. Confusion among them to be mapped land covers is assessed

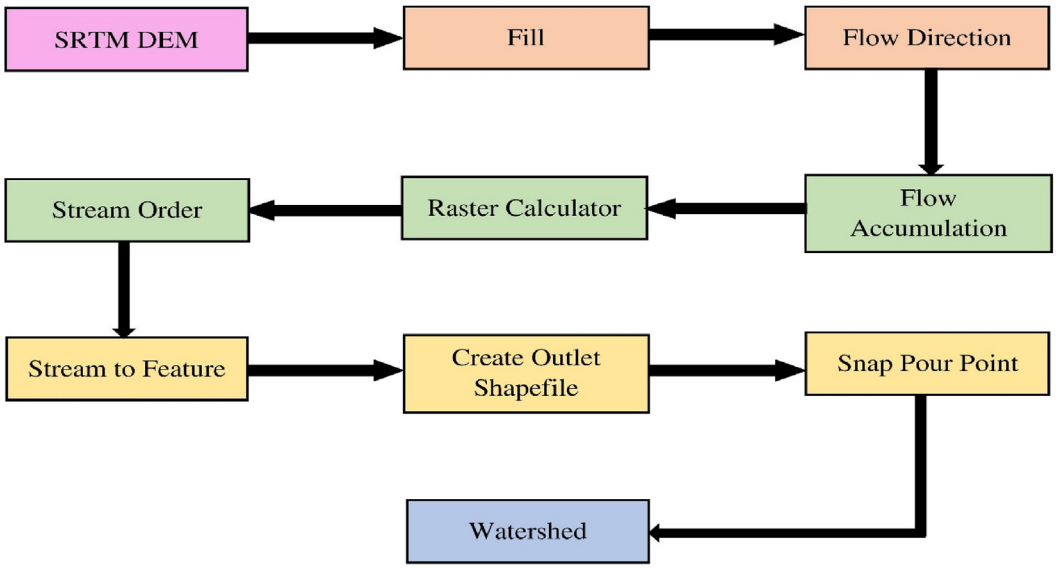

Fig. 2. Murredu watershed delineation flowchart.

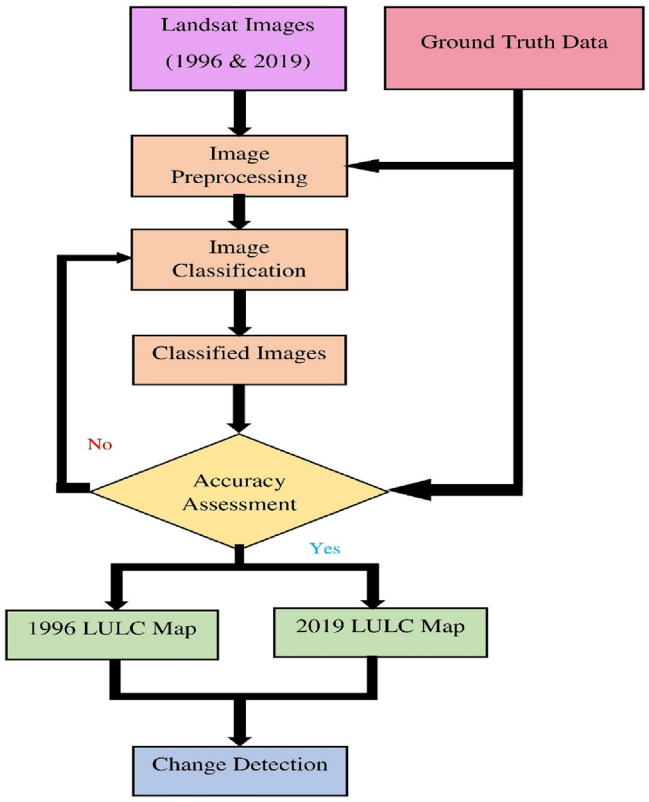

Fig. 3. Murredu Watershed methodological workflow and data analysis.

to be minimal when a spectral signature is deemed to be satisfactory (Gao and Liu, 2010). As a result, using high definition satellite images from Google Earth Pro, signatures were added to the satellite images. After the spectral signature had been determined to be satisfactory, it was added to the classification procedure. After creating a classification system, all the LULC classes were mapped using one of the most used maximum-likelihood methods were applied in this present study.

Table 2
Different types of land cover seen in the Murredu watershed.

LULC category	Description
Barren land	Unforested areas, such as sediments, exposed rocks, landslide zones, degraded forest areas, mined-out land, or excavated surfaces are examples of such areas and so on
Water bodies	Lakes, ponds, rivers, and reservoirs
forest	Forest lands
Built-up	Settlements, artificial infrastructure, transportation and so on
Agricultural	Crop fields and fallow lands

A Google Earth Pro examination has been conducted. To carry out supervised classifications, choose a training site, and assess classification accuracy, ground truth data should be collected. The Google Earth Pro was used to gather training and testing interest sites for the ground truth information in this investigation. The current research area classes were defined after interpretation and five LULC classes (built-up area, agricultural land, forest, barren land, and water-bodies) were identified because the google earth pro image has a high spatial resolution.

5.4. LULC change detection

The LULC mapping project was expected to produce data on the spatial distribution of land use categories, as well as identify and estimate changes in land use over the previous decades. Furthermore, the number of transitions from one land cover category to another between time periods (1996 and 2019) was quantified. Important information about the spatial distribution of LULC changes is presented by the change matrix (Shalaby and Tateishi, 2007). To evaluate the overall changes in LULC classes, a change matrix illustrating the changes in land cover from 1996 to 2019 was created.

5.5. Accuracy assessment

The comparison of a classification with actual data serves as an accuracy assessment, which determines how accurately the classification captures the real world. Using a random sampling

approach with 200 points, an accuracy assessment of the classified images that resulted in this study was done to examine the quality of the information that was produced from the data. The error matrix was used to conduct this evaluation. To assess the degree of classification accuracy from the report portion of ERDAS Imagine 2015, Kappa statistics and the overall accuracy of the categorised images were conducted.

6. Results

6.1. Murredu watershed

This river's watershed covers 1593 km^2 in total (Fig. 4). This watershed had significant LULC changes over time. The resulting LULC from supervised classification is listed in Table 3 and includes five primary classes: built-up area, agricultural land, forest, barren land, and waterbodies for 1996 and 2019, respectively.

6.2. LULC scenario of Murredu watershed, 1996

Agriculture accounted for 54.19 percent of the watershed's land area in 1996. Forest (40.30 %) was the watershed's second most prevalent land cover. Because a forest infiltrates the majority of the rain that falls during the monsoon and reduces both soil erosion and surface runoff, it often plays a significant influence in the hydrological features of a watershed. In low land watersheds, it will also lessen flood intensity (Haque, 2013). As indicated in Fig. 5, at that time, the area was made up of 1.27 % water bodies, 2.80 % of which were occupied by built-up areas, and 1.45 % of bare ground.

6.3. LULC scenario of Murredu watershed, 2019

After 1996, there was a significant amount of deforestation in the watershed region, which left the land unforested and suitable for agriculture and other uses. The majority of the watershed's land was used for agriculture in 2019 (59.36 %). Forest (30.63 %) was the second most prevalent land cover in the watershed. As shown in Fig. 6, the water bodies make up 1.53 % of the total area, while the built-up area occupies almost 3.64 %, and the bare land makes up 4.84 %.

Forests are recognised for promoting groundwater recharge and consuming a lot of water through evapotranspiration from the trees (Aladejana et al., 2018). The deep roots of the forest act as flow pathways to replenish the ground water and raise the base flow (Farinosi et al., 2019). In addition, forest improves the soil's ability to store water and speeds up infiltration (Obahoundje et al., 2018; Zhang et al., 2019). As a result, deforestation reduces the infiltration processes because the soil is less permeable, less rainfall is intercepted, and more runoff, baseflow, and groundwater recharge occur as a result (Naha et al., 2021). In 1996, about 40.30 % of the area was covered by forest, but in 2019, it was

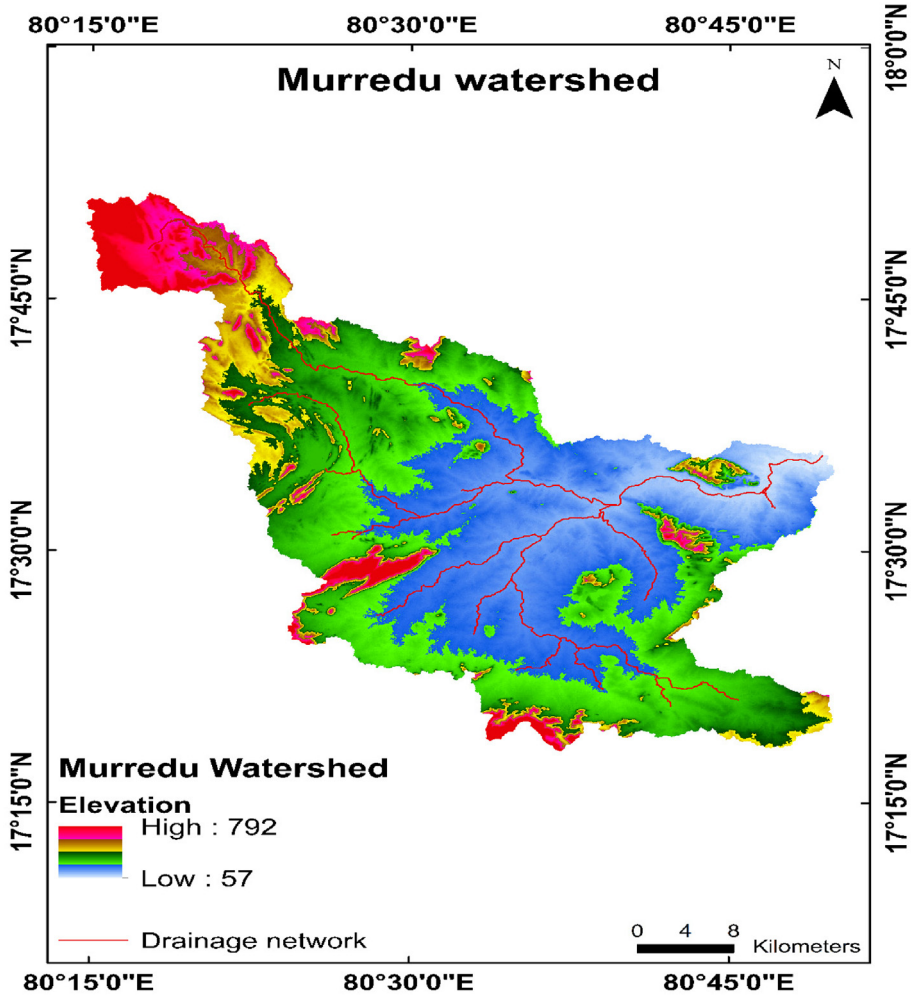

Fig. 4. Delineation of the Murredu watershed's watershed.

Table 3
Distribution of LULC in the Murredu watershed.

LULC Class	1996 Area (km^2)	Area (%)	2019 Area (km^2)	Area (%)
Barren land	23.04	1.45	77.10	4.84
Water-bodies	20.24	1.27	24.40	1.53
Forest	641.94	40.30	487.93	30.63
Built-up Area	44.59	2.80	58.00	3.64
Agricultural Land	863.20	54.19	945.59	59.36
Total	1593.02	100	1593.02	100

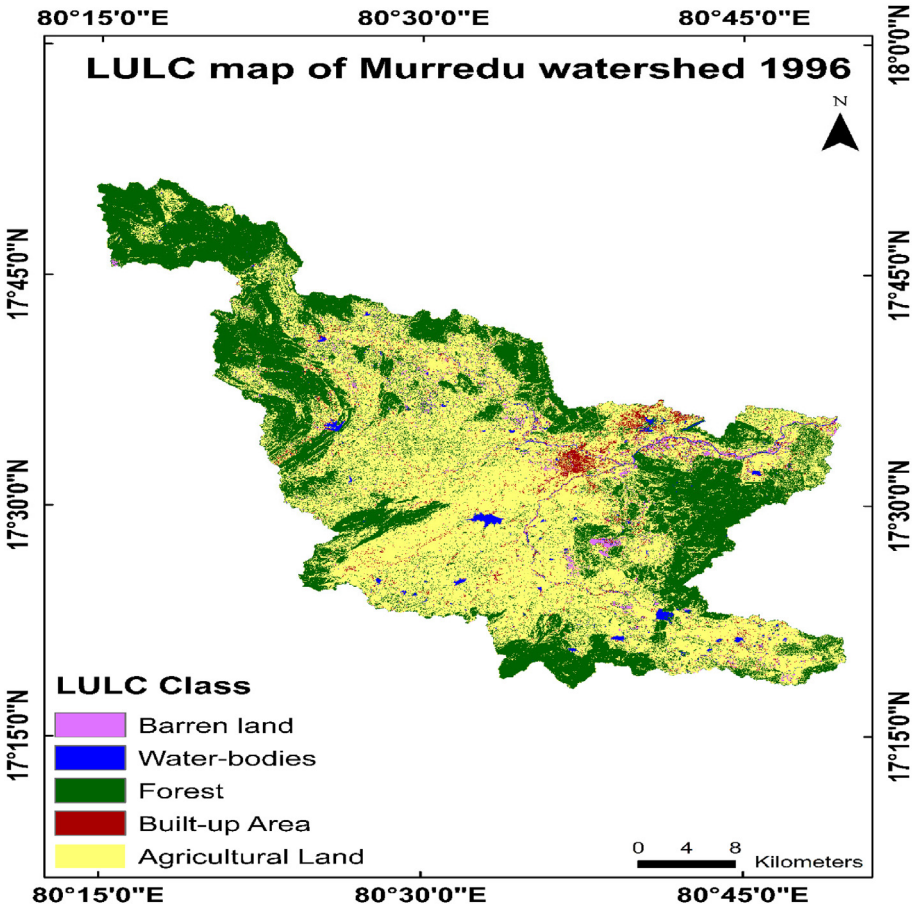

Fig. 5. 1996 map showing the Murredu watershed's LULC.

30.63 %, showing a decrease in forest land. Compared to forests, agricultural lands are more likely to experience higher surface runoff and sediment transportation (Baker and Miller, 2013). On the other side, agriculture is increased from 1996 (54.19 %) to 2019 (59.36 %). Barren land increased from 1996 (1.45 %) to 2019 (4.84 %). Built-up area increased from 1996 (2.80 %) to 2019 (3.64 %) (Table 3). To assess the total changes in LULC classes, a change matrix illustrating the changes in land cover from 1996 to 2019 was created.

6.4. Accuracy assessment

One of the significant differences between the classified image and the actual or real ground is accuracy evaluation. The accuracy of the 2019 classified map was evaluated using one of the most popular Kappa accuracy assessment techniques. Using high-resolution satellite images from Google Earth Pro, 200 stratified random points were generated (Table 4). Accurate assessment of the 1996 image was not possible due to a lack of clear images and their availability. Overall classification accuracy for the classified image of 2019 was found to be 90 % with overall kappa statistics of 85.98 %. Table 5 displays the accuracy of each producer and user for each class.

7. Discussion

7.1. LULC changes

Tables 6 exhibit the LULC change matrix for the years 1996 through 2019 in turn. The numbers in bold indicate that there has been no change in the LULC classes for the specified time frame. The Murredu watershed underwent significant land cover changes over the research period, according to the results of the LULC change matrix. Figs. 7 and 8 show the LULC of the Murredu watershed's temporal pattern and relative variations from 1996 to 2019.

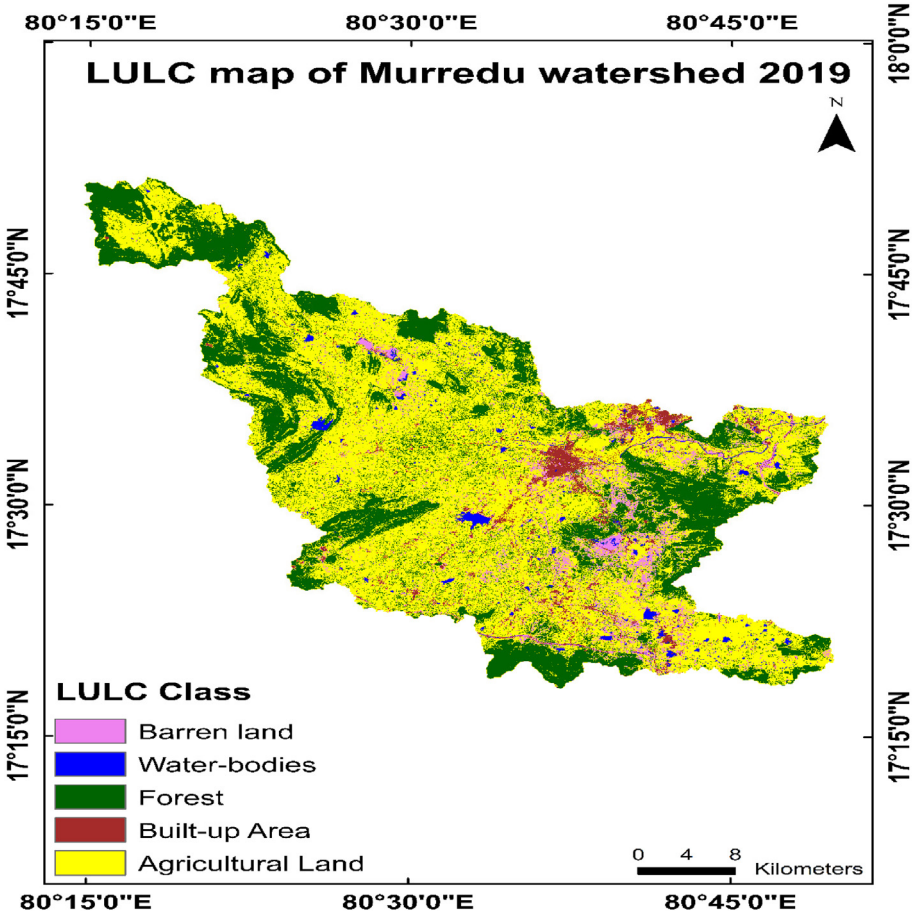

Fig. 6. 2019 map showing the Murredu watershed's LULC.

Table 4
2019 categorised image: Accuracy assessment error matrix.

Reference Data/ Classified Data	Barren land	Water-bodies	Forest	Built-up Area	Agricultural Land	Classified total
Barren land	18	0	0	0	6	24
Water-bodies	1	18	0	1	0	20
Forest	0	0	44	0	7	51
Built-up Area	0	1	0	20	1	22
Agricultural Land	0	0	2	1	80	83
Reference Total	19	19	46	22	94	200

Table 5
2019 categorised image: Producer's and user's accuracy assessment.

LULC Class	Reference Total	Classified Total	Number Correct	Producer's Accuracy	User's Accuracy
Barren land	19	24	18	94.74 %	75.00 %
Water-bodies	19	20	18	94.74 %	90.00 %
Forest	46	51	44	95.65 %	86.27 %
Built-up Area	22	22	20	90.91 %	90.91 %
Agricultural Land	94	83	80	85.11 %	96.39 %

7.2. LULC patterns over the period of 1996–2019

The overall changes from 1996 to 2019 are shown in Table 7. The forest, one of the main land cover classes in this region, has significantly decreased during the past decades. From 1996 to 2019, the area covered by forests decreased by 154.01 km^2. Agriculture is one of the most significant land uses in the basin, second only to forestry, and is another type of land cover in this region. Agriculture has significantly increased during the past decades. From 1996 to 2019, the area covered by forests decreased by 82.38 km^2. Overall, the agricultural area in this watershed increased from 863.20 km^2 (in 1996) to 945.59 km^2 (in 2019).

Table 6
LULC changes matrix as seen in the Murredu watershed between 1996 and 2019.

LULC Class	Barren land	Water-bodies	Forest	Built-up Area	Agricultural Land	Total 2019
Barren land	**5.03**	1.02	13.52	4.43	53.11	77.10
Water-bodies	0.77	**10.72**	3.24	1.20	8.47	24.40
Forest	1.34	1.13	**387.31**	1.90	96.25	487.93
Built-up Area	1.28	1.80	6.14	**13.30**	35.49	58.00
Agricultural Land	14.63	5.57	231.73	23.75	**669.90**	945.59
Total 1996	23.04	20.24	641.94	44.59	863.20	**1593.02**

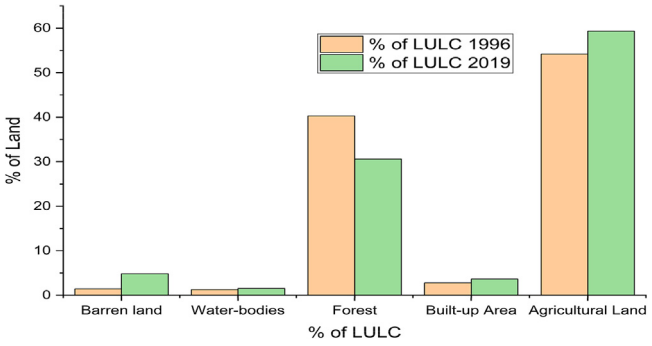

Fig. 7. Temporal patterns in the LULC region of the Murredu watershed.

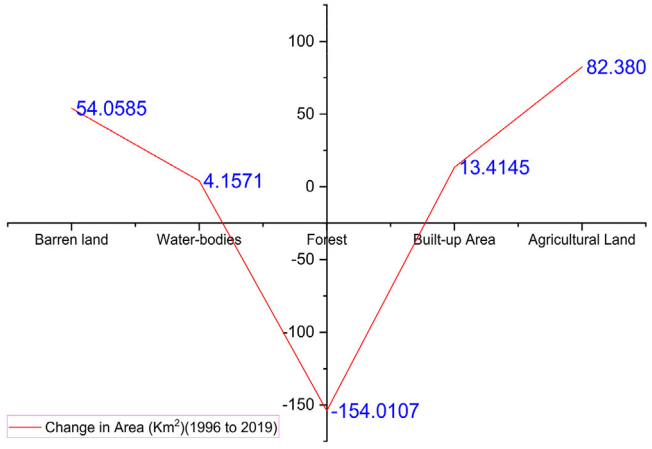

Fig. 8. Diagrammatic representation of kilometres of LULC change in the Murredu basin.

Table 7
Overall changes in LULC classes in each period (Km^2 and %).

LULC Class	Overall changes in 1996–2019 (Km^2)	Overall changes in 1996–2019 (%)
Barren land	54.06	3.39
Water-bodies	4.16	0.26
Forest	−154.01	−9.67
Built-up Area	13.41	0.84
Agricultural Land	82.38	5.17

The shallow water and thick forest along the rivers made it challenging to map water bodies. With 30 m of spatial resolution, the challenge was heightened even more. In 2019, the area covered by water bodies grew. The overall change in waterbodies from 1996 to 2019 is 0.26 %. Overall, the agricultural area in this watershed increased by 5.17 % from 1996 to 2019. Additionally, between 1996 and 2019, the proportion of land that is built-up increased overall by 0.84 %. Between 1996 and 2019, the amount of bare land overall changed by 3.39 %.

8. Conclusion

This present study demonstrates how LULC changes in the Murredu drainage basin have altered significantly over the past decades. Overall classification accuracy for the classified image of 2019 was found to be 90 % with overall kappa statistics of 85.98 %. From these findings, change detection analysis shows that the area used for agricultural land, barren land, forest, built-up areas, and waterbodies has increased by 5.17 %, 3.39 %, 0.84 %, and 0.26 %, respectively, between 1996 and 2019. The forest area has decreased by 9.67 % at the same time. The area of forest has decreased, whereas the areas for agriculture, waterbodies, bare land, and built-up areas have all increased. Therefore, this research anticipates that the findings might provide information to planners, land managers, and decision-makers for the sustainable management and development of the natural resource. In a future study, sub-watersheds could be created within the watershed since it is large enough to be included in management practices. Additionally, these sub-watersheds could be given higher priority for management and conservation based on the degree of deterioration.

Funding

There was no funding for this project.

Data availability statement

The corresponding author will provide the datasets created during and/or analysed during the current investigation upon reasonable request.

CRediT authorship contribution statement

Padala Raja Shekar: Conceptualization, Methodology, Software, Data curation, Writing – original draft. **Aneesh Mathew:** Supervision, Visualization, Investigation, Writing – review & editing.

Declaration of Competing Interest

The authors declare that they have no known competing financial interests or personal relationships that could have appeared to influence the work reported in this paper.

Acknowledgements

The authors would like to thank the editor and anonymous reviewers for their instructive comments, which helped to improve this paper. In addition, the authors wish to thank the U.S. Geological Survey (USGS) for making the satellite data available.

References

Abebe, G., Getachew, D., Ewunetu, A., 2022. Analysing land use/land cover changes and its dynamics using remote sensing and GIS in Gubalafito district, Northeastern Ethiopia. SN Appl. Sci. 4, 30. https://doi.org/10.1007/s42452-021-04915-8.

Akpoti, K., Antwi, E.O., Kabo-bah, A.T., 2016. Impacts of rainfall variability, land use and land cover change on stream flow of the Black Volta Basin, West Africa. Hydrology 3 (3), 26 https://www.mdpi.com/2306-5338/3/3/26.

Aladejana OO, Salami AT, Adetoro OIO (2018) Hydrological responses to land degradation in the Northwest Benin Owena River Basin, Nigeria. J. Environ. Manage. 225, 300-312. https://doi.org/https://doi.org/10.1016/j.jenvman.2018.07.095.

Allan, D., Erickson, D., Fay, J., 1997. The influence of catchment land use on stream integrity across multiple spatial scales. Freshw. Biol. 37 (1), 149–161.

Baker TJ, Miller SN (2013) Using the Soil and Water Assessment Tool (SWAT) to assess land use impact on water resources in an East African watershed. J. Hydrol. 486, 100- 111. https://doi.org/https://doi.org/10.1016/j.jhydrol.2013.01.041.

Belay, T., Mengistu, D.A., 2019. Land use and land cover dynamics and drivers in the Muga watershed, Upper Blue Nile basin, Ethiopia. Remote Sens. Appl. Soc. Environ. 15,. https://doi.org/10.1016/j.rsase.2019.100249 100249.

Chakilu, G., Moges, M., 2017. Assessing the land use/cover dynamics and its impact on the low flow of Gumara Watershed, Upper Blue Nile Basin, Ethiopia. Hydrol. Curr. Res. 7, 2. https://doi.org/10.4172/2157-7587.1000268.

Chen, H., Chen, C., Zhang, Z., Lu, C., Wang, L., He, X., Chu, Y., Chen, J., 2021. Changes of the spatial and temporal characteristics of land-use landscape patterns using multi-temporal Landsat satellite data: A case study of Zhoushan Island China. Ocean Coast. Manag. 213,. https://doi.org/10.1016/j.ocecoaman.2021.105842 105842.

Chen, X., Vierling, L., Deering, D., 2005. A simple and effective radiometric correction method to improve landscape change detection across sensors and across time. Remote Sens. Environ. 98 (1), 63–79.

Coppin, P., Jonckheere, I., Nackaerts, K., Muys, B., Lambin, E., 2004. Digital change detection methods in ecosystem monitoring: a review. Int. J. Remote Sens. 25 (9), 1565e1596.

FAO (1988) Soil Map of the world, Revised Legend with Corrections and Updates World Soil Resource. Food and agricultural organization. FAO, Rome, Italy. Report 60.

Farinosi, F., Arias, M.E., Lee, E., Longo, M., Pereira, F.F., Livino, A., Moorcroft, P.R., Briscoe, J., 2019. Future climate and land use change impacts on river flows in the Tapajós Basin in the Brazilian Amazon. Earth's Future 7 (8), 993–1017.

Gao, J., Liu, Y., 2010. Determination of land degradation causes in Tongyu County, Northeast China via land cover change detection. Int. J. Appl. Earth Obs. Geoinf. 12 (1), 9–16.

Haque, S.M.S., 2013. Watershed Management in Bangladesh. Degradation of Upland Watershed in Bangladesh Project- a USDa Funded Project, Grant No. University of Chittagong (IFESCU), Chittagong 4331, Bangladesh.

Hassaballah, K., Mohamed, Y., Uhlenbrook, S., Biro, K., 2017. Analysis of streamflow response to land use and land cover changes using satellite data and hydrological modelling: case study of Dinder and Rahad tributaries of the Blue Nile (Ethiopia–Sudan). Hydrol. Earth Syst. Sci. 21 (10), 5217–5242. https://doi.org/10.5194/hess-21-5217-2017.

Javed, A., Khanday, M.Y., Ahmed, R., 2009. Prioritization of sub-watersheds based on morphometric and land use analysis using remote sensing and GIS techniques. J. Ind. Soc. Remote Sens. 37 (2), 261–274.

Javed, A., KhandayMY, R.S., 2011. Watershed Prioritization using Morphometric and Land Use Analysis parameters: A Remote Sensing and GIS based approach. J. Geol. Soc. India 78, 63–75.

Kayitesi, N.M., Guzha, A.C., Mariethoz, G., 2022. Impacts of land use land cover change and climate change on river hydro-morphology- a review of research studies in tropical regions. J. Hydrol. 615, 128702.

Kogo, B.K., Kumar, L., Koech, R., 2019. Analysis of spatio-temporal dynamics of land use and cover changes in Western Kenya. Geocarto. Int. 36 (4), 376–391.

Lambin E, Geist H (2006) Land Use, Land Cover Change, Local Process and Global Impacts. Germany: Springer- Verlag Berlin Heidelbrg, Article ISBN-10-3-540-32301- 9. In this issue.

Langat PK, Kumar L, Koech R, Ghosh MK (2020) Characterisation of channel morphological pattern changes and flood corridor dynamics of the tropical Tana River fluvial systems, Kenya. J. Afr. Earth Sci. 163, 103748.

Mathew A and Shekar PR (2023) Flood Prioritization of Basins Based on Geomorphometric Properties Using Morphometric Analysis and Principal Component Analysis: A Case Study of the Maner River Basin. River Dynamics and Flood Hazards. Disaster Resilience and Green Growth. Springer, Singapore. https://doi.org/10.1007/978-981-19-7100-6_18.

Mathew A, Sarwesh P, Khandelwal S (2022) Investigating the contrast diurnal relationship of land surface temperatures with various surface parameters represent vegetation, soil, water, and urbanization over Ahmedabad city in India. Energy Nexus 5:100044.

Meer, M.S., Mishra, A.K., 2020. Land Use / Land Cover changes over a district in northern India using remote sensing and GIS and their impact on society and environment. J. Geol. Soc. India 95 (2), 179–182. https://doi.org/10.1007/s12594-020-1407-2.

Metz, M., Mitasova, H., Harmon, R.S., 2011. Efficient extraction of drainage networks from massive, radar-based elevation models with least cost path search. Hydrol. Earth Syst. Sci. 15, 667–678.

Mohamed, M., Anders, J., Schneider, C., 2020. Monitoring of changes in Land Use/Land cover in Syria from 2010 to 2018 using multitemporal Landsat imagery and GIS. Land 9 (7), 226.

Nagendra, H., Pareeth, S., Ghate, R., 2006. People within parks-forest villages, land-cover change and landscape fragmentation in the Tadoba Andhari Tiger Reserve, India. Appl. Geogr. 26 (2), 96–112.

Nageswara Rao, P.V., Appa Rao, S., Subba Rao, N., 2018. Delineation of groundwater prospective zones from a delta region of India, using geoelectrical and water quality approach. Environ. Earth Sci. 77, 616. https://doi.org/10.1007/s12665-018-7786-7.

Naha, S., Rico-Ramirez, M.A., Rosolem, R., 2021. Quantifying the impacts of land cover change on hydrological responses in the Mahanadi river basin in India. Hydrol. Earth Syst. Sci. 25 (12), 6339–6357. https://doi.org/10.5194/hess-25-6339-2021.

Obahoundje, S., Diedhiou, A., Ofosu, E.A., Anquetin, S., François, B., Adounkpe, J., Amoussou, E., Kouame, Y.M., Kouassi, K.L., Nguessan, B.V.H., Youan, T.M., 2018. Assessment of Spatio-Temporal Changes of Land Use and Land Cover over South-Western African Basins and Their Relations with Variations of Discharges. Hydrology 5 (4), 56 https://www.mdpi.com/2306-5338/5/4/56.

Rai, S.C., Sharma, E., Sundriyal, R.C., 1994. Conservation in the Sikkim Himalaya: traditional knowledge and land-use of the Mamlay watershed. Environ. Conserv. 21 (1), 30–34. https://doi.org/10.1017/s0376892900024048.

Rao, N.S., Chakradhar, G.K.J., Srinivas, V., 2001. Identification of Groundwater Potential Zones Using Remote Sensing Techniques in and Around Guntur Town, Andhra Pradesh, India. J. Ind. Soc. Remote Sens. 29 (1-2), 69–78.

Rawat, J.S., Kumar, M., 2015. Monitoring land use/cover change using remote sensing and GIS techniques: a case study of Hawalbagh block, district Almora, Uttarakhand, India. Egypt. J. Rem. Sens. Space Sci. 18, 77–84.

Redvan, G., Mustafa, U., 2021. Flood prioritization of basin based on geomorphometric properties using principal component analysis, morphometric analysis and Redvan's priority methods: a case study of Harshit river basin. J. Hydrol. https://doi.org/10.1016/j.jhydrol.2021.127061.

Santillan JR, Amora AM, Makinano-Santillan M, Gingo AL, Marqueso JT (2019) Analyzing the impacts of land cover change to the hydrologic and hydraulic behaviours of the Philippines' third largest River Basin. ISPRS Ann. Photogramm. Remote Sens. Spatial Inf. Sci., IV-3/W1, 41-48. https://doi.org/10.5194/isprs-annals-IV-3-W1- 41-2019.

Schulz, J.J., Cayuela, L., Echeverria, C., Salas, J., Rey Benayas, J.M., 2010. Monitoring land cover change of the dryland forest landscape of Central Chile (1975e2008). Appl. Geogr. 30 (3), 436e447.

Serra, P., Pons, X., Saurí, D., 2008. Land-cover and land-use change in a Mediterranean landscape: a spatial analysis of driving forces integrating biophysical and human factors. Appl. Geogr. 28 (3), 189–209.

Shalaby, A., Tateishi, R., 2007. Remote sensing and GIS for mapping and monitoring land cover and landuse changes in the Northwestern coastal zone of Egypt. Appl. Geogr. 27 (1), 28–41. https://doi.org/10.1016/j.apgeog.2006.09.004.

Shekar PR, Mathew A (2022c) Prioritising sub-watersheds using morphometric analysis, principal component analysis, and land use/land cover analysis in the Kinnerasani River basin, India. H2Open J. 5 (3): 490–514. doi: https://doi.org/10.2166/h2oj.2022.017.

Shekar PR and Mathew A (2023) Erosion Susceptibility Mapping Based on Hypsometric Analysis Using Remote Sensing and Geographical Information System Techniques. River Dynamics and Flood Hazards. Disaster Resilience and Green Growth. Springer, Singapore. https://doi.org/10.1007/978-981-19-7100-6_26.

Shekar, P.R., Mathew, A., 2022a. Mathew A (2022a) Morphometric analysis for prioritizing sub-watersheds of Murredu River basin, Telangana State, India, using a geographical information system. J. Eng. Appl. Sci. 69 (1). https://doi.org/10.1186/s44147-022-00094-4.

Shekar, P.R., Mathew, A., 2022b. Mathew A (2022b) Evaluation of Morphometric and Hypsometric analysis of the Bagh River basin using Remote Sensing and Geographic Information System techniques. Energy Nexus 7, 100104.

Singh, A., 1989. Digital change detection techniques using remotely-sensed data. Int. J. Remote Sens. 10 (6), 989e1003.

Subba Rao, N., 2003. Groundwater prospecting and management in an agro-based rural environment of crystalline terrain of India. Environ. Geol. 43, 419–431. https://doi.org/10.1007/s00254-002-0659-z.

Subba Rao, N., 2006. Groundwater potential index in a crystalline terrain using remote sensing data. Environ. Geol. 50 (7), 1057–1067 https://doi. org/10.1007/s00254-006-0280-7.

Subba Rao, N., 2009. A numerical scheme for groundwater development in a watershed basin of basement terrain: A case study from IndiaUn procédé numérique pour la viabilisation des eaux souterraines dans un bassin versant sur des terrains du socle: étude de cas en IndeUn esquema numérico para el desarrollo de las aguas subterráneas en una cuenca hidrográfica en basamento: un caso de estudio de la India基岩地区流域盆地地下水开发的一种数值方法：一个印度的实例研究Uma metodologia numérica para o planeamento da água subterrânea numa bacia hidrográfica em terrenos de soco cristalino: um caso de estudo na Índia. Hydrgeol. J. 17 (2), 379–396.

Subba Rao, N., 2011. Guidelines for success of well site selections. Curr. Sci. 100 (8), 1119–1120.

Subba Rao, N., 2012. Indicators for occurrence of groundwater in the rocks of Eastern Ghats. Curr. Sci. 103 (4), 352–353 https://www.jstor.org/stable/24085075.

Subba Rao, N., Prathap Reddy, R., 2004. Geoenvironmental appraisal in a developing urban area. Environ. Geol. 47 (1), 20–29. https://doi.org/10.1007/s00254-004-1122-0.

Subba Rao, N., Moeen, S., Surya Rao, P., Dinakar, A., Nageswara Rao, P.V., Sunitha, B., Rudra, D., Srinivasu, N., 2016. Morphometric approach using remote sensing and GIS in watershed management. J. Appl. Geochem. 18 (1), 45–56.

Subba Rao, N., Sakram, G., Rashmirekha, D., 2022. Deciphering artificial groundwater recharge suitability zones in the agricultural area of a river basin in Andhra Pradesh, India using geospatial techniques and analytical hierarchical process method. Catena 212,. https://doi.org/10.1016/j.catena.2022. 106085 106085.

Teklay A, Dile YT, Asfaw DH, Bayabil HK, Sisay K (2021) Impacts of Climate and Land Use Change on Hydrological Response in Gumara Watershed, Ethiopia. Ecohydrol. Hydrobiol. 21(2), 315-332. https://doi.org/https://doi.org/10.1016/j.ecohyd.2020.12.001.

Tian, H., Banger, K., Bo, T., Dadhwal, V.K., 2014. History of land use in India during 1880–2010. Large scale land transformations reconstructed from satellite data and historical archives. Global Planet Change 121, 78–88.

Wubie, M.A., Assen, M., Nicolau, M.D., 2016. Patterns, causes and consequences of land use/cover dynamics in the Gumara watershed of lake Tana basin, Northwestern Ethiopia. Environ. Syst. Res. Springer Open J. 5, 12.

Wulder, M.A., White, J.C., Goward, S.N., Masek, J.G., Irons, J.R., Herold, M., Cohen, W.B., Loveland, T.R., Woodcock, C.E., 2008. Landsat continuity: Issues and opportunities for land cover monitoring. Remote Sens. Environ. 112 (3), 955–969.

Wyman, M.S., Stein, T.V., 2010. Modeling social and land-use/land-cover change data to assess drivers of smallholder deforestation in Belize. Appl. Geogr. 30 (3), 329e342.

Yang, X., Lo, C.P., 2002. Using a time series of satellite imagery to detect land use and land cover changes in the Atlanta, Georgia metropolitan area. Int. J. Remote Sens. 23 (9), 1775–1798.

Zhang, D., Wang, Z., Guo, Q., Lian, J., Chen, L., 2019. Increase and Spatial Variation in Soil Infiltration Rates Associated with Fibrous and Tap Tree Roots. Water 11 (8), 1700 https://www.mdpi.com/2073-4441/11/8/1700.